J|A|C|S
ARTICLES
Published on Web 08/11/2005

Model Electrochemical-Mass Spectrometric Studies of the Cytochrome P450-Catalyzed Oxidations of Cyclic Tertiary Allylamines

Ulrik Jurva,[†] Philippe Bissel,[‡] Emre M. Isin,[‡] Kazuo Igarashi,[‡] Simon Kuttab,[‡,§] and Neal Castagnoli, Jr.*,[‡]

Contribution from the Department of DMPK and Bioanalytical Chemistry, AstraZeneca R&D Mölndal, S-431 83 Mölndal, Sweden, and the Department of Chemistry, Virginia Tech, Blacksburg, Virginia 24061-0212

Received March 31, 2005; E-mail: ncastagn@vt.edu

Abstract: Single-electron transfer and hydrogen atom transfer pathways have been proposed to account for the cytochrome P450-catalyzed α-carbon oxidations of amines. With the aid of electrochemistry-electrospray ionization mass spectrometry, the electrochemical potentials required for the one-electron oxidations of *N*-methyl- and selected *N*-cyclopropyl-4-phenyl-1,2,3,6-tetrahydropyridinyl derivatives and the chemical fates of the resulting aminyl radical cations have been investigated. Comparison of the results of these studies with those observed in the corresponding enzyme catalyzed oxidations suggests that aminyl radical cations are not obligatory intermediates in the cytochrome P450-catalyzed α-carbon oxidations of this class of substrates.

Introduction

The mechanism by which amines undergo cytochrome P450 (cP450)-catalyzed α-carbon oxidation has been[1] and continues to be[2] a topic of interest. Scheme 1 summarizes two pathways that have been proposed for this overall two-electron oxidation. The single-electron transfer (SET) pathway involves an initial transfer of one electron from the nitrogen lone pair of the substrate (**1**) to the cP450-activated iron-oxo system (Fe^{V}═O → Fe^{IV}═O).[1a−e,2a,c,f,g] Proton transfer from the resulting aminyl radical cation $\mathbf{1}^{\bullet+}$ (coupled to Fe^{IV}═O → Fe^{III}—OH) is proposed to lead to the carbon radical $\mathbf{2}^{\bullet}$. The second one-electron oxidation proceeds via radical recombination (oxygen rebound) to give the Fe^{III} resting state of cP450 and an equilibrium mixture of the α-carbinolaminium species $\mathbf{3H}^{+}$ and iminium species $\mathbf{4}^{+}$. The second pathway, involving an initial hydrogen atom transfer (HAT) from the α-carbon atom of the substrate to the iron-oxo system (Fe^{V}═O → Fe^{III}—OH), gives carbon radical intermediate $\mathbf{2}^{\bullet}$ without passing through the aminyl radical cation $\mathbf{1}^{\bullet+}$.[2b,d,e]

The cP450 mechanism-based inactivator properties of *N*-benzylcyclopropylamine (**5**) are consistent with the SET pathway (Scheme 2).[3] The strained cyclopropyl group of the aminyl radical cation $\mathbf{5}^{\bullet+}$, when in the bisected conformation,[4] is proposed to open to generate the distonic radical cation $\mathbf{6}^{\bullet+}$. This primary carbon radical is thought to form a covalent adduct ($\mathbf{7H}^{+}$) with an active site functionality of the enzyme. A critical experiment in support of this proposal established that the 1-methylcyclopropyl analogue **8**, which cannot undergo the HAT reaction, still inactivated the enzyme.[1c,d] This behavior may be rationalized by a reaction sequence ($\mathbf{8} \rightarrow \mathbf{8}^{\bullet+} \rightarrow \mathbf{9}^{\bullet+} \rightarrow \mathbf{10H}^{+}$) analogous to that proposed for *N*-benzylcyclopropylamine ($\mathbf{5} \rightarrow \mathbf{5}^{\bullet+} \rightarrow \mathbf{6}^{\bullet+} \rightarrow \mathbf{7H}^{+}$). Based on these results, the cP450-catalyzed oxidations of amines should proceed via the sequence $\mathbf{1} \rightarrow \mathbf{1}^{\bullet+} \rightarrow \mathbf{2}^{\bullet} \rightarrow \mathbf{3H}^{+}$ (Scheme 1).

Recent evidence challenging SET as an exclusive pathway for the cP450-mediated oxidations of amines has been provided from studies on *N*-cyclopropyl-*p*-chloroaniline derivatives bearing *N*-methyl and *N*-isopropyl groups.[5] The salient outcomes of this study include the following: (1) replacement of the C(1)-cyclopropyl proton with a methyl group shifts the product composition from a mixture of the *N*-dealkylated and *N*-decyclopropylated metabolites to the *N*-dealkylated metabolites

[†] AstraZeneca R&D Mölndal.
[‡] Virginia Tech.
[§] Current address: Birzeit University, Department of Chemistry, Birzeit, West Bank, Via Israel.

(1) (a) Guengerich, F. P.; Willard, R. J.; Shea, J. P.; Richards, L. E.; Macdonald, T. L. *J. Am. Chem. Soc.* **1984**, *106*, 6446. (b) Hanzlik, R. P.; Tullman, R. H. *J. Am. Chem. Soc.* **1982**, *104*, 2048. (c) Macdonald, T. L.; Zirvi, K.; Burka, L. T.; Peyman, P.; Guengerich, F. P. *J. Am. Chem. Soc.* **1982**, *104*, 2050. (d) Augusto, O.; Beilan, H. S.; Ortiz de Montellano, P. R. *J. Biol. Chem.* **1982**, *257*, 11288. (e) Bondon, A.; Macdonald, T. L.; Harris, T. M.; Guengerich, F. P. *J. Biol. Chem.* **1989**, *264*, 1988. (f) Tullman, R. H.; Hanzlik, R. P. *Devel. Biochem. Drug Action Des.: Mech. Based Enzymol. Inhib.* **1979**, *6*, 187.
(2) (a) Sato, H.; Guengerich, F. P. *J. Am. Chem. Soc.* **2000**, *122*, 8099. (b) Manchester, J. I.; Dinnocenzo, J. P.; Higgins, L. A.; Jones, J. P. *J. Am. Chem. Soc.* **1997**, *119*, 5069. (c) Guengerich, F. P.; Yun, C. H.; Macdonald, T. L. *J. Biol. Chem.* **1996**, *271*, 27321. (d) Karki, S. G.; Dinnocenzo, J. P.; Jones, J. P.; Korzekwas, K. R. *J. Am. Chem. Soc.* **1995**, *117*, 2732. (e) Dinnocenzo, J. P.; Karki, S. B.; Jones, J. P. *J. Am. Chem. Soc.* **1993**, *115*, 7111. (f) Guengerich, F. P.; Bell, L. C.; Okazaki, O. *Biochimie* **1995**, *77*, 573. (g) Guengerich, F. P.; Okazaki, O.; Seto, Y.; Macdonald, T. L. *Xenobiotica* **1995**, 689. (h) Miwa, G. T.; Walsh, J. S.; Kedderis, G. L.; Hollenberg, P. F. *J. Biol. Chem.* **1983**, *258*, 14445. (i) Hall, L. R.; Hanzlik, R. P. *J. Biol. Chem.* **1990**, *265*, 12349.
(3) Hanzlik, R. P.; Kishore, V.; Tullman, R. *J. Med. Chem.* **1979**, *22*, 759.
(4) Tidwell, T. T. *The Chemistry of the Cyclopropyl Group*; John Wiley & Sons: New York, 1987; pp 565−622.
(5) Bhakta, M. N.; Wimalasena, K. *J. Am. Chem. Soc.* **2002**, *214*, 1844.

10.1021/ja052048o CCC: $30.25

Scheme 1

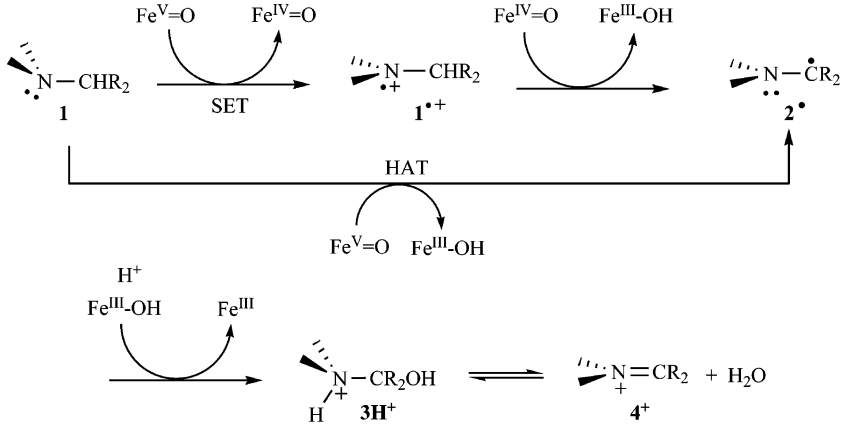

Scheme 2

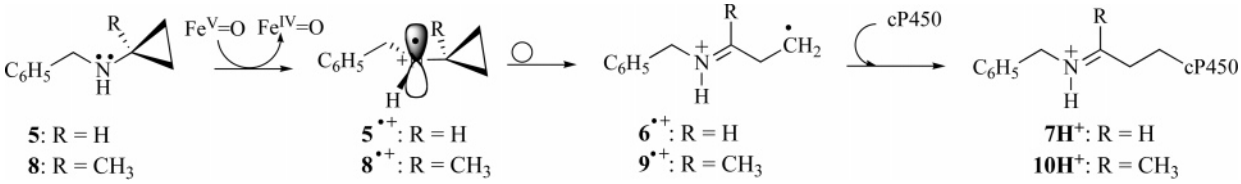

Scheme 3

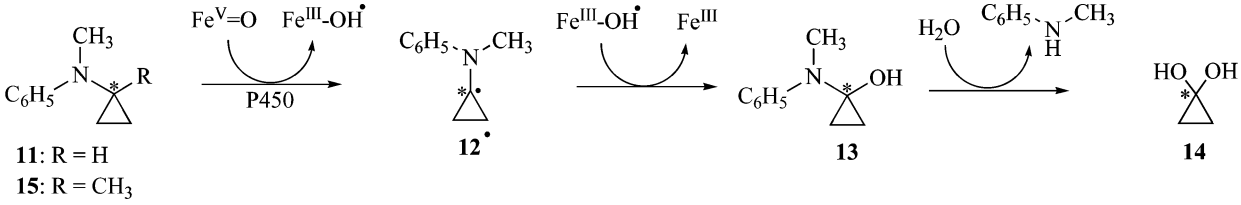

exclusively; (2) replacement of the C(1)-cyclopropyl proton with a deuteron leads to a shift in product composition to favor *N*-dealkylated metabolites ($k_H/k_D = 3.1 \pm 0.1$); and (3) a model SET reaction, using $Fe^{3+}(Phen)_3(PF_6^-)_3$ as a one-electron oxidant, overwhelmingly favors, in all cases, the *N*-decyclopropylation pathway which presumably proceeds via ring opened intermediates. The authors conclude that an SET mechanism can account for these observations only if the rate of the isotope sensitive α-carbon deprotonation of the aminyl radical cation is much faster than the rate of opening of the cyclopropyl ring.

Results from Hanzlik's laboratory have provided direct evidence that cP450-catalyzed oxidations of amines may proceed via an HAT pathway.[6] In this study cyclopropanone hydrate (**14**) was characterized as a cP450-generated metabolite of the ^{13}C-labeled *N*-methyl-*N*-phenylcyclopropylaminyl analogue **11**. Convincing evidence to support the intermediacy of the HAT carbon radical **12**• included the observation that the α-methyl analogue **15** did not undergo cP450-catalyzed decyclopropylation. Radical recombination of **12**• with the heme-stabilized hydroxyl group followed by cleavage of the resulting α-carbinolamine **13** led to cyclopropanone hydrate (**14**) that was identified by ^{13}C NMR spectroscopy (Scheme 3). Thus, 1-methylcyclopropylaminyl substrates have provided evidence supporting both the SET and the HAT mechanism.

Studies from our laboratory have focused on the monoamine oxidase-[7] and cP450-catalyzed[8] α-carbon oxidations of various 1,4-disubstituted 1,2,3,6-tetrahydropyridinyl derivatives. Members of this class of compounds, including the parkinsonian inducing neurotoxin 1-methyl-4-phenyl-1,2,3,6-tetrahydropyridine [MPTP (**16**)], are biotransformed via ring allylic α-carbon oxidation. In the case of MPTP, the pyridinium metabolite **18**$^+$, formed via the dihydropyridinium intermediate **17H**$^+$, is thought to mediate the neurodegenerative properties of the parent compound.[9] As part of these studies we have examined the cP450-mediated oxidation of 1-cyclopropyl- (**19**), *trans*-1-(2-methylcyclopropyl)- (**20a**),[10] and *trans*-1-(2-phenylcyclopropyl)- (**21**) 1,2,3,6-tetrahydropyridine with phenobarbital induced rat liver microsomes and expressed forms of cP450 3A4 and cP450 2D6.[11] All three preparations converted these substrates to the corresponding dihydropyridinium and pyridinium metabolites (**19** → **22H**$^+$ → **25**$^+$; **20a** → **23H**$^+$ → **26**$^+$; and **21** → **24H**$^+$ →

(6) (a) Shaffer, C. L.; Harriman, S.; Koen, Y. M.; Hanzlik, R. P. *J. Am. Chem. Soc*. **2002**, *124*, 8268. (b) See also Bissel, P.; Castagnoli, N., Jr.; Penich, S. *Bioorg. Med. Chem.* **2005**, *13*, 2975.

(7) Bissel, P.; Bigley, M. C.; Castagnoli, K.; Castagnoli, N., Jr. *Bioorg. Med. Chem*. **2002**, *10*, 3031. Kalgutkar, A. S.; Castagnoli, N., Jr. *J. Med. Chem*. **1992**, *35*, 4165. Wang, Y. X.; Castagnoli, N., Jr. *J. Med. Chem*. **1995**, *38*, 1904. Yu, J.; Castagnoli, N., Jr. *Bioorg. Med. Chem*. **1999**, *7*, 2835.

(8) Ottoboni, S.; Carlson, T. J.; Trager, W. F.; Castagnoli, K.; Castagnoli, N., Jr. *Chem. Res. Toxicol.* **1990**, *3*, 423.

(9) Royland, J. E.; Langston, J. W. *Highly Selective Neurotoxins. Basic and Clinical Applications;* Humana Press: New Jersey 1998; pp 141−194.

(10) The synthetic approach to the 2-methylcyclopropyl analogue led to the formation of a mixture of the trans (**20a**) and cis (**20b**, not shown) isomers which were separated by column chromatography (see Experimental Section).

(11) (a) Zhao, Z.; Mabic, S.; Kuttab, S.; Franot, C.; Castagnoli, K.; Castagnoli, N., Jr. *Bioorg. Med. Chem*. **1998**, *6*, 2531. (b) Kuttab, S.; Shang, J.; Castagnoli, N., Jr. *Bioorg. Med. Chem*. **2001**, *9*, 1685. (c) Shang, X. MS Thesis, Virginia Tech, 1999.

Scheme 4

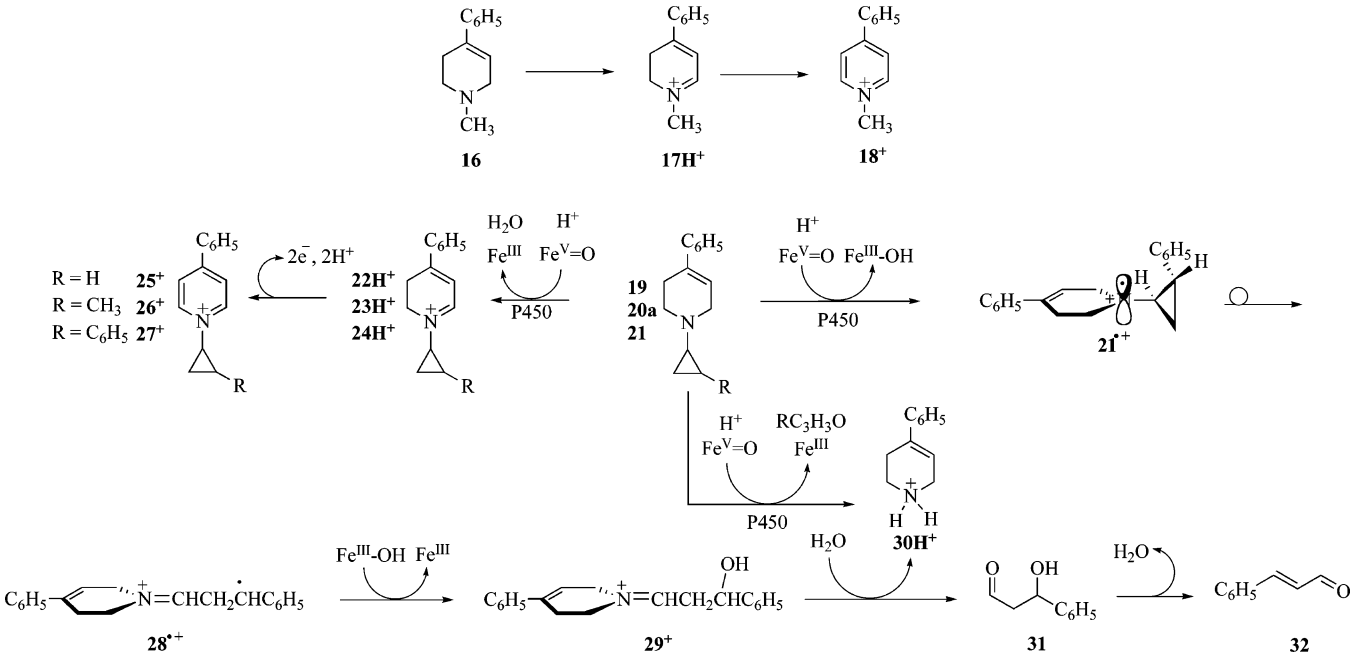

27$^+$) and to the 4-phenyl-1,2,3,6-tetrahydropyridinium product **30H**$^+$. Although the fates of the cyclopropyl group present in **19** and **20a** were not determined, the phenylcyclopropyl group present in **21** was converted, at least in part, to cinnamaldehyde (**32**). We have interpreted the cP450-catalyzed conversion of **21** to **30H**$^+$ + **32** as evidence supporting the SET pathway since a plausible sequence leading to these products would proceed via **21**$^{\bullet+}$ → **28**$^{\bullet+}$ → **29**$^+$ → **30H**$^+$ + **31** and **31** → **32** as shown in Scheme 4. It is not known if this is a route unique to **21** and/or if decyclopropylation of **19** and **20a** also proceed via an analogous SET pathway.

We also have examined the oxidation of MPTP, the 1-cyclopropyl- (**19**) and related 1-cyclopropyl-4-substituted 1,2,3,6-tetrahydropyridinyl analogues of MPTP in acetonitrile by the 1-electron oxidant $Fe^{3+}(Phen)_3(PF_6^-)_3$.[12] MPTP was converted rapidly and exclusively to the pyridinium species **18**$^+$ (see Scheme 4) whereas none of the 1-cyclopropyl analogues underwent ring allylic α-carbon oxidation.

It is difficult to accommodate all of the experimental results summarized above exclusively in terms of the SET or the HAT mechanism. The conversion of the *trans*-1-(2-phenylcyclopropyl) analogue **21** to cinnamaldehyde (**32**) is best rationalized by the SET mechanism, while the conversion of *N*-methyl-*N*-phenylcyclopropylamine (**11**) to cyclopropanone hydrate (**14**) is best rationalized in terms of the HAT pathway. In the present report we describe the results of our attempts to characterize by electrospray ionization/mass spectrometry (ESI/MS) the fate of aminyl radical cations that have been generated by electrochemical (EC) oxidation. If SET is an obligatory pathway for the cP450-catalyzed oxidations of tertiary amines, then one might anticipate that the electrochemically generated cyclopropylaminyl radical cations would be converted, at least to some extent, in this model reaction to the corresponding dihydropyridinium products that are formed in the enzyme-catalyzed reactions. On-line monitoring by ESI/MS of substrate disappearance also provides an opportunity to investigate the influence of *N*-substituents on the electrochemical potential required to form aminyl radical cations. In contrast to the $Fe^{3+}(Phen)_3(PF_6^-)_3$ model reactions, these EC oxidations are carried out in aqueous MeOH, providing an opportunity to observe single-electron chemical events under protic-polar conditions that resemble more closely those present in an enzyme active site. As with any model reaction, however, one must assume that restrictions imposed by the enzyme active site do not exclude chemical events that are observed in the solution reaction.

Results and Discussion

Studies of the on-line coupling of electrochemistry and mass spectrometry in the field of drug metabolism date back to 1986.[13] The evolution of these studies has led to instrumentation that provides on-line coupled EC-ESI/MS capabilities with considerable versatility and sensitivity.[14] In the present study, the EC-ESI/MS technique has been exploited to provide information on the fates of the aminyl radical cations generated by the one-electron oxidations of the *N*-substituted tetrahydropyridinyl derivatives **16**, **19**, **20a**, and **21**. The procedure involves pumping a solution of the substrate through a porous graphite electrochemical cell while the potential of the cell is ramped from 0 to 1500 mV. The perfusate then enters the mass spectrometer. The positively charged species (MH^+ and M^+) of the substrates and oxidation products generated under ESI conditions are monitored on-line by MS, and mass voltammograms (MVs) are constructed by plotting the resulting integrated ion intensities vs potential. The oxidation products generated by passing a solution of the substrate molecule through the electrochemical cell held at an appropriate constant potential can be characterized by LC-ESI/MS and product ion spectral analyses. Additionally the influence of substituents on the oxidation potentials of the

(12) Franot, C.; Mabic, S.; Castagnoli, N., Jr. *Bioorg. Med. Chem.* **1998**, *6*, 283.

(13) Hambitzer, G.; Heitbaum, J. *Anal. Chem.* **1986**, *58*, 1067. Getek, A. Proceedings of the 34th ASMS Annual Conference on Mass Spectrometry and Allied Topics, Cincinnati, 1986.

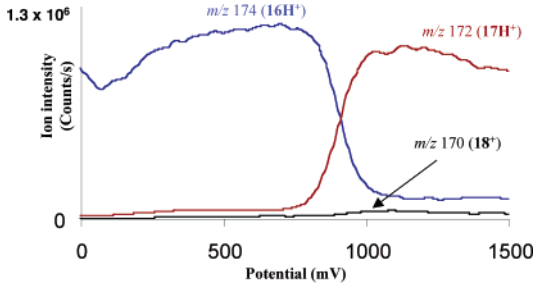

Figure 1. Mass voltammograms of MPTP (**16H**$^+$) and its oxidation products **17H**$^+$ and **18**$^+$.

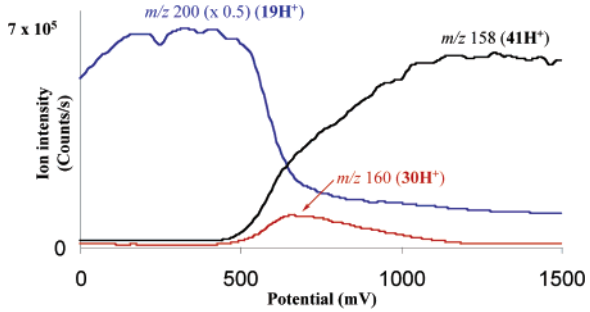

Figure 2. Mass voltammograms of the cyclopropyl analogue **19H**$^+$ and its oxidation products **30H**$^+$ and **41H**$^+$. For clarity, the intensity of the ion at *m*/*z* 200 has been divided by 2.

substrates can be estimated by comparing the potentials at which the ion intensities (MH$^+$ values) of the starting substrates start to decline.

The MVs obtained with MPTP are shown in Figure 1. At approximately 700 mV the intensity of the MH$^+$ ion of MPTP at *m*/*z* 174 started to decrease and was replaced by a species at *m*/*z* 172. At higher potentials, a weak signal was detected at *m*/*z* 170. An ion at *m*/*z* 160 also was present at trace levels. Comparison of the LC-ESI/MS tracings and product ion spectra (PIS) obtained of the compounds generated following oxidation of MPTP at 950 mV with synthetic standards confirmed that MPTP had undergone oxidation first to the dihydropyridinium species **17H**$^+$ (*m*/*z* 172) that subsequently was converted at higher potentials to the pyridinium species **18**$^+$ (*m*/*z* 170). The structure of the compound present at trace levels was shown to be the *N*-demethylated secondary aminium species **30H**$^+$ (*m*/*z* 160, Scheme 5).

These results are rationalized by the pathways shown in Scheme 5 in which the one-electron oxidation product **16**$^{\bullet+}$ of MPTP undergoes preferential α-carbon deprotonation at the C-6 allylic position to give the α-carbon radical **33**$^\bullet$. Following a second one-electron oxidation, **33**$^\bullet$ is converted to the dihydropyridinium species **17H**$^+$. A minor route proceeds via deprotonation of the methyl substituent of **16**$^{\bullet+}$ to give carbon radical **34**$^\bullet$ that is oxidized to the exocyclic iminium intermediate **35**$^+$. Hydrolytic cleavage of **35**$^+$ generates the secondary aminium species **30H**$^+$. The predominance of allylic ring α-carbon oxidation reflects the greater acidity of the allylic C-6 proton relative to the *N*-methyl proton of the aminyl radical cation **16**$^{\bullet+}$. The gas-phase energies for the formation of the corresponding conjugate bases **33**$^\bullet$ and **34**$^\bullet$ from **16**$^{\bullet+}$, when calculated at the Unrestricted Hartree−Fock (UHF) level of theory[15] using the 6-31G* basis set, gave ΔE (**34**$^\bullet$) − ΔE (**33**$^\bullet$) = 29.6 kcal/mol.[16] The corresponding values when calculated by density functional theory (DFT)[17] using the pBP[18] model with the DN** basis set and the SVWN[19] model with the DN** basis set were 24.5 and 25.5 kcal/mol, respectively. The results of all three computational methods predict the selective ring allylic oxidation observed in this experiment. These results are consistent with the SET pathway for the enzyme-catalyzed oxidation of MPTP to its dihydropyridinium species **17H**$^+$, a known rat cP450 1A1 metabolite of MPTP.[8] On the other hand, the human cP450 2D6-catalyzed α-carbon oxidation of MPTP leads principally to the *N*-demethylated metabolite **30H**$^+$,[20] a product that cannot be readily rationalized by the SET pathway.

The MVs obtained with the *N*-cyclopropyl analogue **19** show that the intensity of the parent ion at *m*/*z* 200 starts to decline at about 450 mV and is replaced by a species detected at *m*/*z* 160 (Figure 2). This product undergoes further oxidation to give a species detected at *m*/*z* 158. A signal too weak to be observed in Figure 2 also was detected at higher potentials at *m*/*z* 156.[21] A careful search for ions at *m*/*z* 198 and 196, corresponding to the MH$^+$ values for the known dihydropyridinium and pyridinium species **22H**$^+$ and **25**$^+$, respectively, failed. When subjected to EC-MS analysis both **22H**$^+$ and **25**$^+$ proved to be stable at up to 1000 mV. Consequently, it is likely that these two compounds would have been detected had they been formed following the one-electron oxidation of **19**. The LC-ESI/MS and PIS obtained from the reaction mixture generated at 500 mV confirmed the structures of the *N*-decyclopropylated secondary aminium species **30H**$^+$ (*m*/*z* 160), the corresponding dihydropyridinium species **41H**$^+$ (*m*/*z* 158),[22] and the pyridinium species **42**$^+$ (*m*/*z* 156).

These results may be rationalized by assuming the rapid ring opening of the electrochemically generated cyclopropylaminyl radical cation **19**$^{\bullet+}$ to yield the distonic radical cation **37**$^{\bullet+}$ (Scheme 6). A second one-electron oxidation of **37**$^{\bullet+}$ leads to the eniminium species **38**$^+$ that undergoes hydrolytic cleavage to form the *N*-dealkylated product **30H**$^+$ and an unidentified product equivalent to a C_3H_4O unit. Compound **30H**$^+$ proved to be unstable at 500 mV and underwent oxidation to the corresponding dihydropyridinium species **41H**$^+$ that, in turn, was oxidized, at higher potentials, to the pyridinium species **42**$^+$.

(14) Volk, K. J.; Yost, R.; Brajter-Toth, A. *Anal. Chem.* **1992**, *64*, 21A. Zhou, F.; Berkel, G. J. V. *Anal. Chem.* **1995**, *67*, 3643. Liu, X.; Cole, R. B. *Anal. Chem.* **1997**, *69*, 2478. Regino, M. C. S.; Brajter-Toth, A. *Anal. Chem.* **1997**, *69*, 5067. Diehl, G.; Liesener, A.; Karst, U. *Analyst* **2001**, *126*, 288. Jurva, U.; Wikström, H. V.; Weidolf, L.; Bruins, A. P. *Rapid Commun. Mass Spectrom.* **2003**, *17*, 800. Jurva, U.; Wikström, H. V.; Bruins, A. P. *Rapid Commun. Mass Spectrom.* **2002**, *16*, 1934. Permentier, H. P.; Jurva, U.; Barroso, B.; Bruins, A. P. *Rapid Commun. Mass Spectrom.* **2003**, *17*, 1585.
(15) Hartiharan, P. C.; Pople, J. A. *Theor. Chim. Acta* **1973**, *28*, 213.
(16) See Experimental Section for a description of the computational methods used.
(17) Hohenberg, P.; Kohn, W. *Phys. Rev.* **1964**, *136*, B864. Kohn, W.; Sham, L. J. *Phys. Rev.* **1965**, *140*, A1133.
(18) Becke, A. D. *Phys. Rev. A* **1988**, *38*, 3089. Perdew, J. P. *Phys. Rev. B* **1986**, *33*, 8822.
(19) Vosko, S. H.; Wilk, L.; Nusair. M. *Can. J. Phys.* **1980**, *58*, 1200.
(20) Di Monte, D.; Shinka, T.; Sandy, M. S.; Castagnoli, N., Jr.; Smith, M. T. *Drug Metab. Dispos.* **1988**, *16*, 250. Narimatsu, S.; Tachibana, M.; Masubuchi, Y.; Suzuki, T. *Chem. Res. Toxicol.* **1996**, *9*, 93. Coleman, T.; Ellis, W.; Martin, I. J.; Lennard, M. S.; Tucker, G. T. *J. Pharmacol. Exp. Ther.* **1996**, *277*, 685.
(21) It should be noted that additional oxidation products at higher masses also were detected. The characterization of these compounds, as well as those observed with the other cyclopropylamines discussed in this paper, will be reported separately.
(22) A synthetic sample of **41H**$^+$ was not available. The structure assignment was made by showing that the PIS of the EC generated ion at *m*/*z* 158 was identical to the corresponding ion generated by the EC oxidation of 4-phenyl-1,2,3,6-tetrahydropyridine (**30**).

Scheme 5

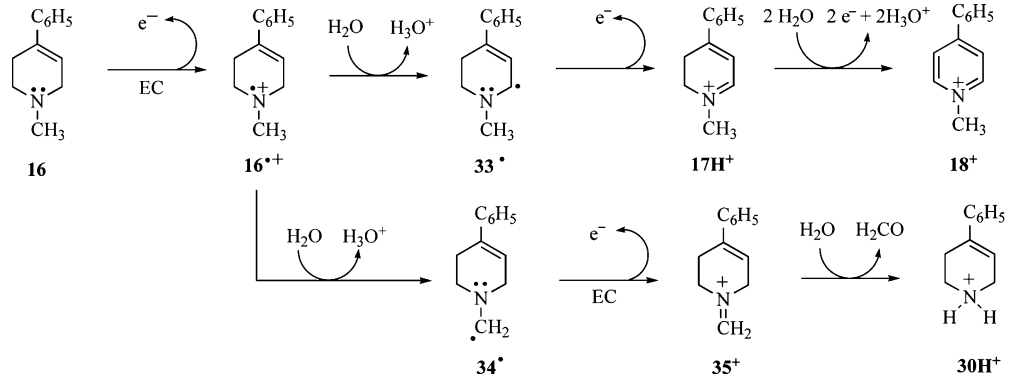

Scheme 6

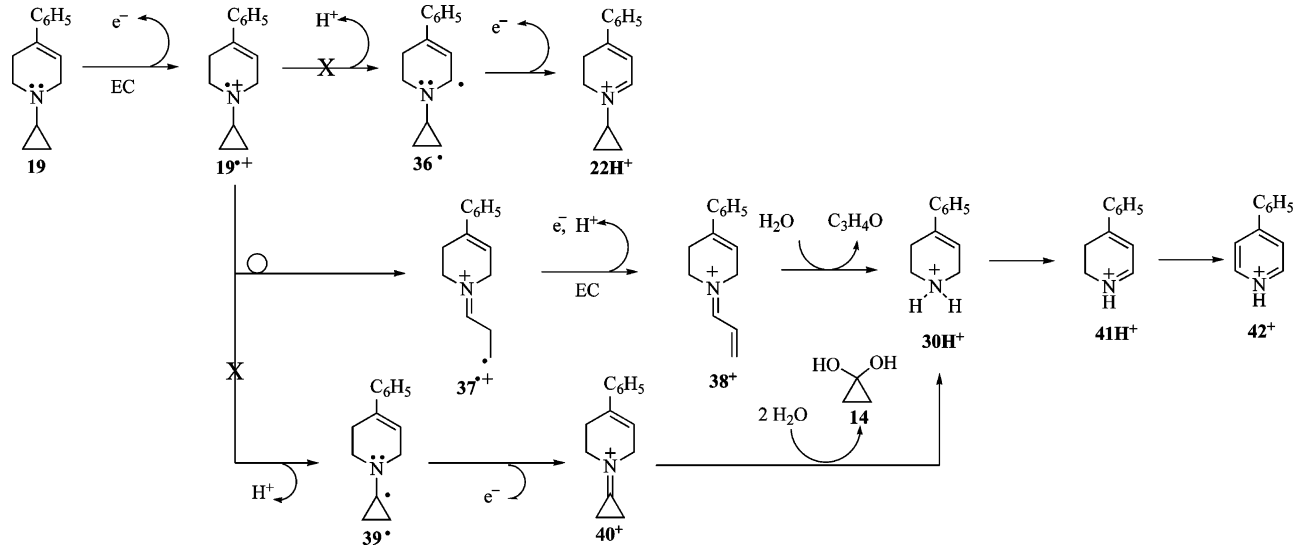

An alternative proposal to account for the *N*-decyclopropylation pathway involves deprotonation of the cyclopropylaminyl radical cation **19**$^{\bullet+}$ to give **39**$^{\bullet}$, a radical intermediate analogous to that proposed by Hanzlik to account for the cP450-mediated formation of cyclopropanone hydrate (**14**) from *N*-methyl-*N*-phenylcyclopropylamine (Scheme 3). In the present case, a second one-electron transfer and hydrolytic cleavage of the resulting iminium intermediate **40**$^{+}$ would generate **30H**$^{+}$ and cyclopropanone hydrate (**14**). This alternative pathway (**19**$^{\bullet+}$ → **39**$^{\bullet}$ → **40**$^{+}$ → **14** + **30H**$^{+}$), however, is not favored energetically. The calculated differences in gas-phase energies of the allylic radical **36**$^{\bullet}$ (the conjugate base of the allylic C(6)−H acid of **19**$^{\bullet+}$) and the corresponding cyclopropylmethide radical **39**$^{\bullet}$ (the conjugate base of the cyclopropylmethide C−H acid of **19**$^{\bullet+}$) are 31.9 (UHF/6-31G*), 27.8 (DFT/pBP/DN**), and 30.0 kcal/mol (DFT/SVWN/DN**), all in favor of **36**$^{\bullet}$. Consequently, the preference for the ring allylic carbon oxidation, a pathway not observed in this experiment, should be favored by orders of magnitude over oxidation of the cyclopropylmethide carbon.

The MVs obtained with the *trans*-1-(2-methylcyclopropyl) analogue **20a** and *trans*-(2-phenylcyclopropyl) analogue **21** also show that the loss of the parent ion is linked to the formation of the secondary aminium species **30H**$^{+}$ that, subsequently, is converted to the dihydropyridinium species **41H**$^{+}$. The pyridinium species **42**$^{+}$ also is observed at higher potentials.

Scheme 4 above presents the two cP450-mediated oxidation pathways for **19**, **20a**, and **21**. One pathway leads to the dihydropyridinium (**22H**$^{+}$, **23H**$^{+}$, and **24H**$^{+}$) and pyridinium (**25**$^{+}$, **26**$^{+}$, and **27**$^{+}$) metabolites and the other to the secondary aminium product **30H**$^{+}$ and, in the case of **21**, to cinnamaldehyde. The results obtained with the EC-ESI/MS study show that all three cyclopropylamines are converted principally to the secondary aminium product **30H**$^{+}$, presumably via the corresponding cyclopropylaminyl radical cations, distonic radical cations, and eniminium species (Scheme 7). The expected ion corresponding to the MH^{+} value of cinnamaldehyde, which has a poor ionization efficiency, was not detected in the EC-ESI/MS study of the phenylcyclopropyl analogue **21**. Confirmation of the formation of cinnamaldehyde in this reaction, however, was obtained by LC-diode array analysis of the reaction mixture generated by the oxidation of **21** at 120 mV. The retention times in two different mobile phases (2.16 and 3.25 min) and the UV spectrum (λ_{max} 278 nm) of the product obtained with the reaction mixture were identical to those observed with a synthetic standard. Consequently, the proposed EC reaction pathway for **21** (**21** → **21**$^{\bullet+}$ → **28**$^{\bullet+}$ → **45**$^{+}$ → **30H**$^{+}$ + **32**) is analogous to the cP450-catalyzed pathway (**21** → **21**$^{\bullet+}$ → **28**$^{\bullet+}$ → **29**$^{+}$ → **30H**$^{+}$ + **32**) proposed to account for the conversion of **21** to **30H**$^{+}$ + **32**.

Although ions corresponding to the pyridinium species **25**$^{+}$, **26**$^{+}$, and **27**$^{+}$ were not observed in the mass spectra of the EC

Scheme 7

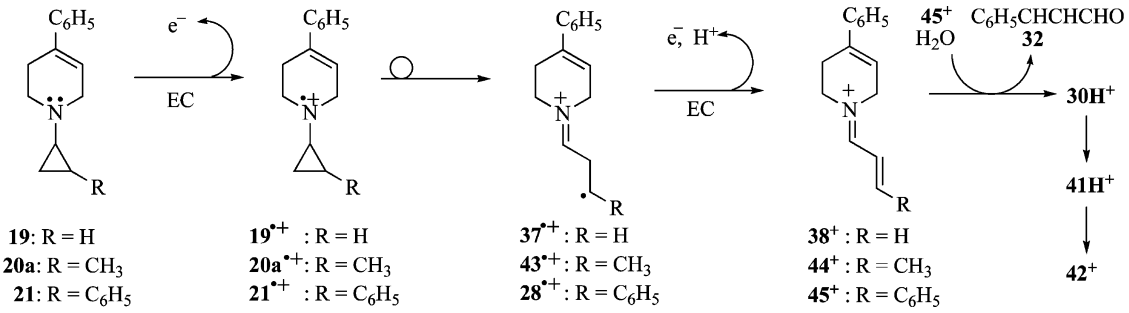

Scheme 8

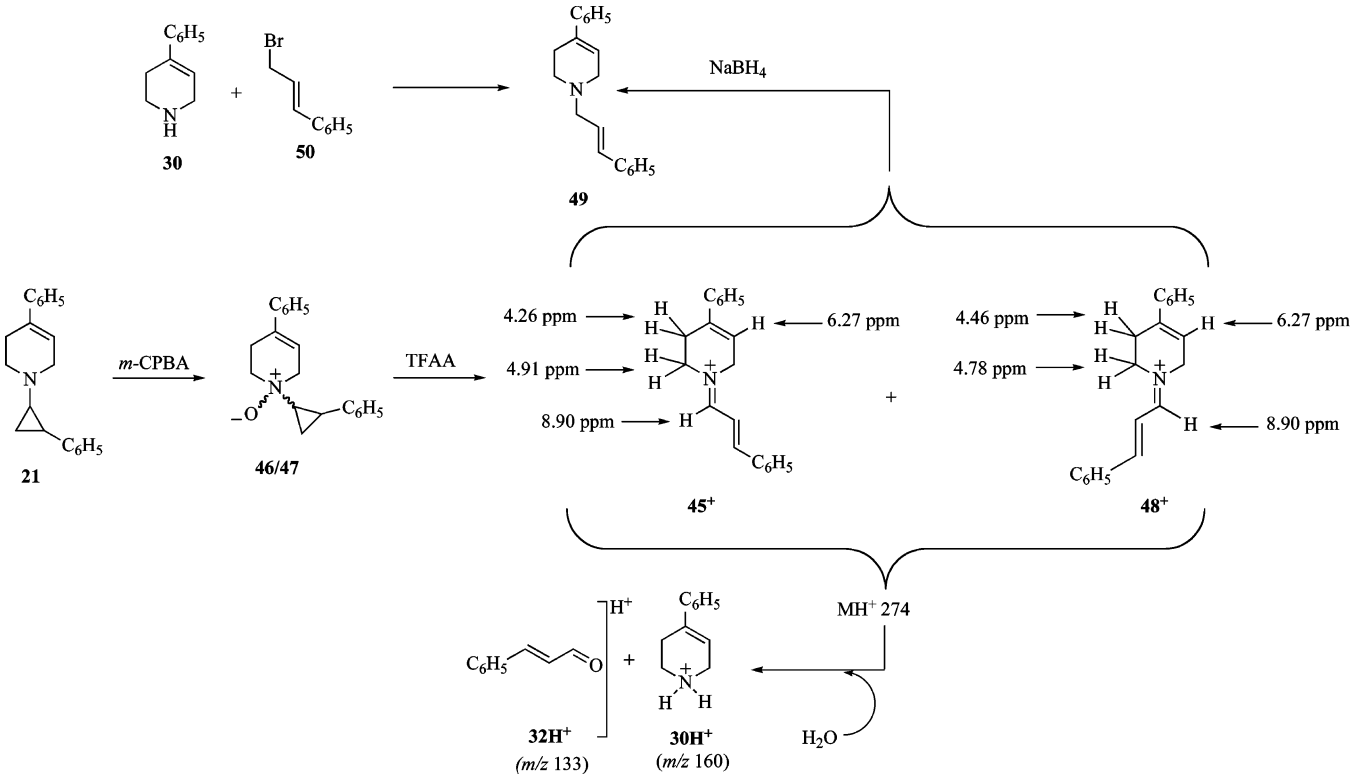

generated oxidation products derived from **19**, **20a**, and **21**, respectively, a weak signal at *m*/*z* 274, the nominal mass for the phenylcyclopropyldihydropyridinium species **24H**$^+$, was detected. An even weaker signal was observed at *m*/*z* 212 corresponding to the methylcyclopropyldihydropyridinium species **23H**$^+$. Attempts to synthesize **24H**$^+$ were initiated in an effort to determine if this cyclic iminium species is formed following electrochemical one-electron oxidation of **21**.

The syntheses of 1,4-disubstituted dihydropyridinium derivatives have been achieved by treatment of the corresponding *N*-oxide intermediates with trifluoroacetic anhydride (TFAA).[11a] This reaction (Scheme 8) was attempted with the diastereomeric mixture of *N*-oxides (**46**/**47**) obtained by treatment of **21** with *m*-chloroperoxybenzoic acid (*m*-CPBA). ESI/MS of the product displayed the expected MH$^+$ ion at *m*/*z* 274. Upon standing in aqueous MeOH containing 10 mM ammonium formate, however, this ion was replaced with an ion at *m*/*z* 160. Comparison of the PIS of this ion with the PIS of a synthetic standard established its structure as the 4-phenyl-1,2,3,6-tetrahydropyridinium species **30H**$^+$. Furthermore, LC diode array analysis established the presence of cinnamaldehyde (**32**) in the mixture. This behavior was not consistent with the dihydropyridinium compound **24H**$^+$ but was consistent with the eniminium species **45**$^+$, the putative intermediate in the EC oxidation of the tetrahydropyridinyl analogue **21**. The ^{1}H NMR spectrum of the analytically pure product confirmed this speculation. The spectrum was readily interpreted in terms of a product consisting of a 3/2 mixture of the cis/trans eniminium isomers **45**$^+$/**48**$^+$. Diagnostic signals (arbitrary configurational assignments) are shown in Scheme 8. As observed in the ESI/MS and diode array analyses, addition of water to a DMSO-d_6 solution of the product resulted in the quantitative hydrolysis of the eniminium derivatives to the secondary aminium species **30H**$^+$ and cinnamaldehyde (**32**). Finally, treatment of **45**$^+$/**48**$^+$ with $NaBH_4$ gave the expected tertiary amine **49** that was synthesized independently from the secondary amine **30** and cinnamyl bromide (**50**). The coupling constant for the olefinic protons (J = 20 Hz) corresponded to the trans structure **49** which rules out a cis configuration for this double bond in the eniminium mixture. GC-EI/MS analysis of the reduction reaction mixture showed a single peak and confirmed that none of the isomeric tetrahydropyridinyl compound **21**, which would be formed by reduction of the dihydropyridinium species **24H**$^+$, was present.

Scheme 9

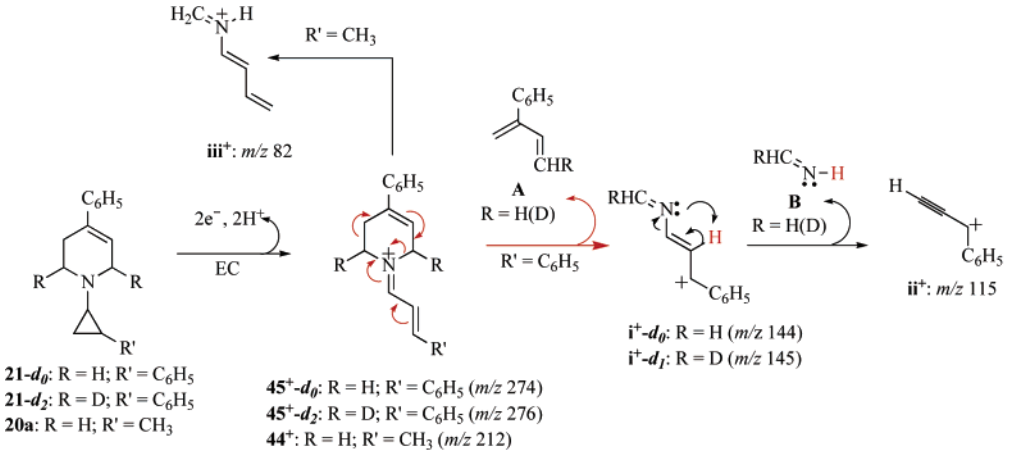

The PIS (MH^+, *m*/*z* 274) of the synthetic diastereomeric mixture **45**$^+$/**48**$^+$ and of the product formed by EC oxidation of **21-*d*$_0$** (presumably the same cis/trans mixture) were essentially identical. Two principal fragment ions, *m*/*z* 144 (100%) and 115 (60%), were observed in these spectra (Scheme 9). Initial fragmentation to give **i**$^+$**-*d*$_0$** (*m*/*z* 144) is accompanied by the neutral loss of 2-phenyl-1,3-butadiene (**A**). Subsequent neutral loss of methyleneimine (**B**) from the phenyl ethynyl carbinyl cation **i**$^+$**-*d*$_0$** gives **ii**$^+$ (*m*/*z* 115). The PIS obtained with **45**$^+$**-*d*$_2$** (*m*/*z* 276) generated in the EC-ESI/MS of **21H**$^+$**-*d*$_2$** (*m*/*z* 278) confirmed these assignments.[23] As required, the mass of the ion at *m*/*z* 144 (**i**$^+$**-*d*$_0$**) shifted to *m*/*z* 145 (**i**$^+$**-*d*$_1$**), while the mass of **ii**$^+$ at *m*/*z* 115 was unchanged. These results establish unambiguously the assignment of the species with MH^+ at *m*/*z* 274 observed at low levels in the EC-ESI/MS of **21** as the hydrolytically unstable eniminium intermediates **45**$^+$/**48**$^+$ that are formed by the pathway presented in Scheme 7. Although we could not obtain a pure sample of the corresponding methyleniminium species **44**$^+$, the PIS of the EC-generated species (*m*/*z* 212) from the methylcyclopropyl analogue **20a** gave a single major fragment ion at *m*/*z* 82 (Scheme 9). This ion corresponds in mass to the fragment ion at *m*/*z* 144 observed in the PIS of synthetic **45**$^+$/**48**$^+$ and the EC-generated eniminium species derived from the phenylcyclopropyl analogue **21**. Unlike the ion at *m*/*z* 144, the ion at *m*/*z* 82 does not fragment further to lose methyleneimine (**B**), presumably because its structure is the stable dienylmethyleniminium species **iii**$^+$. These results provide convincing evidence that the cyclopropylaminyl radical cations formed following one-electron oxidation of cyclopropyltetrahydropyridinyl derivatives undergo rapid ring opening to the corresponding distonic radical cations. No evidence could be obtained for the ring α-carbon oxidation pathway.

From a review of the redox potentials of the four tertiary amines examined in this study it is evident that the ease of EC oxidation is dependent on the *N*-substituent. To obtain a more accurate estimate of the initial potentials at which each compound undergoes EC oxidation, the MVs were obtained using a mixture containing equimolar concentrations of all four compounds (Figure 3).

The *N*-methyl compound (**16**) undergoes initial oxidation at a higher potential (650 mV) than does the *N*-cyclopropyl analogue **19** (350 mV). The *trans*-2-methylcyclopropyl analogue **20a** undergoes initial oxidation at an even lower potential (240 mV), while the *trans*-2-phenylcyclopropyl analogue **21** undergoes initial oxidation at the lowest potential (40 mV). Gas-phase energy calculations provide insight into the factors responsible for these shifts in redox potential. The vertical ionization potentials (IP_v) of the substrates were calculated at the Hartree−Fock (HF)[16] and UHF levels of theory with the 6-31G* basis set. These calculations show that, when no nuclear motion is allowed, the energies required to remove one electron from the nitrogen lone pairs are similar for all four compounds (Table 1). On the other hand, the corresponding adiabatic ionization potentials (IP_a), calculated for the geometry-optimized aminyl radical cations, show a clear trend [6.33 (**16**), 6.03 (**19**), 5.91 (**20a**), and 4.74 eV (**21**)] that is consistent with the observed redox potentials. Perhaps even more informative are the calculated bond distances of the cyclopropylaminyl radical cations after geometry optimization (Table 1). Modest increases in the lengths of the C1−C2 bond are observed for the aminyl radical cations **19**$^{\bullet+}$ and **20a**$^{\bullet+}$ derived from the proteo (**19**) and methyl (**20a**) analogues. In the case of the phenyl analogue **21**, the C1−C2 bond length of the putative phenylcyclopropyl radical cation **21**$^{\bullet+}$ is calculated to be 2.43 Å. These results suggest that the lower redox potentials associated with the one-electron oxidations of the cyclopropylaminyl analogues **19** and **20a** compared to the *N*-methylaminyl analogue **16** reflect lowered activation energies leading to the corresponding cyclopropylaminyl radical cations **19**$^{\bullet+}$ and **20a**$^{\bullet+}$ that are achieved through partial rupture of the cyclopropyl C1−C2 bonds and release of ring strain energy. In the case of the phenylcyclo-

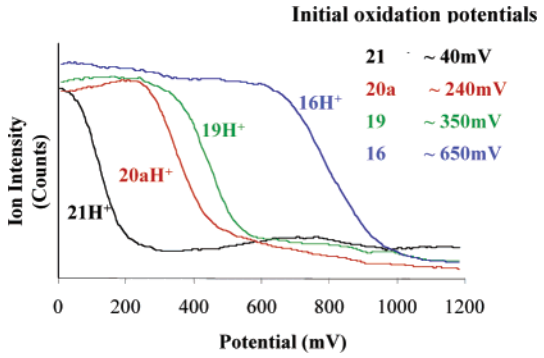

Figure 3. Mass voltamograms for **16H**$^+$, **19H**$^+$, **20aH**$^+$, and **21H**$^+$ obtained with a mixture of the substrates. For clarity, the ion intensities have been normalized to approximately 100% at 0 mV.

(23) The absence of an ion at *m*/*z* 275 [corresponding to the dihydropyridinium product that would be generated by α-carbon oxidation of **21** with loss of the C(6) hydrogen atom] is consistent with the radical cation **21**$^{\bullet+}$ undergoing ring opening exclusively.

Table 1. Observed Initial Aminyl Substrate Oxidation Potentials and Calculated Ionization Potentials and Bond Lengths for Aminyl Substrates and Corresponding Radical Cations

substrate/ radical cation	initial oxidation potential[a]	IP_V (eV)	IP_A (eV)	bond lengths (Å) of the geometry optimized substrates and radical cations							
				aminyl substrates				aminyl radical cations			
				N−C1	C1−C2	C2−C3	C1−C3	N−C1	C1−C2	C2−C3	C1−C3
16/**16**$^{\bullet+}$	650	7.00	6.33	1.44				1.45			
19/**19**$^{\bullet+}$	350	6.97	6.03	1.43	1.49	1.50	1.50	1.42	1.53	1.48	1.50
20a/**20a**$^{\bullet+}$	240	6.97	5.91	1.43	1.50	1.50	1.50	1.41	1.54	1.48	1.52
21/**21**$^{\bullet+}$	40	6.95	4.74	1.43	1.50	1.50	1.50	1.27	2.43	1.51	1.50

[a] The potential at which the ion intensity of the substrate started to decline.

propyl analogue **21**, there appears to be no energy barrier for ring opening; instead, **21** proceeds directly to the distonic radical cation **28**$^{\bullet+}$ without passing through a discrete cyclopropylaminyl radical cation intermediate. These data provide a rationale to account for the observed fates of the four compounds following EC oxidation. They also support the proposal that the cP450-catalyzed ring α-carbon oxidations of cyclopropylamines **19**, **20a**, and **21** do not proceed via the SET pathway.

Summary and Conclusion

The results presented in this paper are consistent with those of several recent studies on the chemistry and metabolism of cyclopropylamines. Although EPR signals attributable to cyclopropylaminyl radical cations are observed in frozen matrices at temperatures below 130 K,[24] compelling evidence argues that these highly unstable species ring open at extremely rapid rates at more elevated temperatures.[5,12,25] Computational analyses support this behavior. Removal of an electron from the lone pair of cyclopropylamine is accompanied by ring opening.[26] Accordingly, the aminyl radical cation of cyclopropylamine is not located in an energy minimum in the radical cation potential energy surface. The calculations reported in the present paper indicate partial ring opening of the aminyl radical cations derived from the cyclopropylaminyl and methylcyclopropylaminyl analogues **19** and **20a** and complete rupture of the ring upon one-electron loss from the phenylcyclopropyl derivative **21**.

We conclude that aminyl radical cations are unlikely to be obligatory intermediates in the cP450-catalyzed ring α-carbon oxidations of *N*-cyclopropyl cyclic tertiary allylamines. Rather, an HAT pathway, analogous to that proposed for the oxidative *N*-decyclopropylation of *N*-methyl-*N*-phenylcyclopropylamine (**11**, Scheme 3), will be preferred. The catalytic pathway(s) accounting for the cP450-catalyzed α-carbon oxidation of other amine substrates remain(s) to be determined.

Experimental Section

General Methods. Compounds **16**•HCl, **30**•HCl, and **32** were purchased from Aldrich. Compounds **17H**$^+$**·ClO$_4^-$**,[27] **18**$^{+\bullet}$**I**$^-$,[28] **19H**$^+$**·HOOCCOO**$^-$,[29] **21H**$^+$**·HOOCCOO**$^-$,[11b] **22H**$^+$**·ClO$_4^-$**,[11a] and **25**$^+$**·ClO$_4^-$**[27] and **46**/**47**[11b] were synthesized as described previously. THF was distilled from sodium and benzophenone. Proton and ^{13}C NMR spectra were recorded on a JEOL 500-MHz spectrometer. A 400 MHz INOVA spectrometer was used for the NOE experiment. The HPLC analyses of cinnamaldehyde were performed on an Agilent 1100 HPLC system equipped with a UV/vis diode array detector (G1328B) using a Zorbax XDB-C8 column (4.6 mm × 150 mm, 5 μm) with an XDB-C8 guard column filter (2.1 mm × 12.5 mm, 5 μm) and acetonitrile/water (56:44 and 30:70) as the mobile phase at a flow rate of 1 mL/min and an injection volume of 20 μL. The GC-EI/MS analysis was performed on a Hewlett-Packard 6890 gas chromatography fitted with an HP-1 capillary column (15 m × 0.2 mm i.d., 0.33 mm film thickness), which was coupled to a Hewlett-Packard 5870 mass-selective detector. Data were acquired using an HP 5970 Chemstation.

Molecular Modeling Calculations. Molecular modeling calculations were carried out using MacSpartan Pro software (Version 1.0.4; Wave function, Irvine, CA). Geometry optimizations were initiated at the semiempirical AM1 level of theory. Final geometry optimizations and energy calculations were carried out at HF or, for radicals, at UHF level of theory with the 6-31G* basis set. The convergence criteria for geometry optimizations were the maximum gradient components reaching <0.002 hartree. The differences in energies of the C-6 allylic radicals **33**• [from MPTP (**16**)] and **36**• (from the cyclopropyl analogue **19**) vs the corresponding methylene radical **34**• and the cyclopropylmethide radical **39**• were estimated by deleting the appropriate proton from each of the radical cations **16**$^{\bullet+}$ and **19**$^{\bullet+}$, respectively, and calculating the energy of the resulting neutral radicals following geometry optimization. Single-point energies of the HF or UHF geometry-optimized molecules also were calculated using the DFT/pBP and DFT/SVWN models with the DN** numerical basis set. Vertical ionization potentials (IP_v) were calculated as follows: the energies of the geometry-optimized amines **16**, **19**, **20a**, and **21** were calculated. Single-point energy calculations were carried out on the radical cations (**16**$^{\bullet+}$, **19**$^{\bullet+}$, **20a**$^{\bullet+}$, and **21**$^{\bullet+}$) using the same geometry as the corresponding amines. The differences in energies are reported as the IP_v. The adiabatic ionization potentials (IP_a) were calculated as the difference in energy between the geometry-optimized amines and the corresponding geometry-optimized aminyl radical cations.

EC-ESI/MS System. The EC-ESI/MS system was setup as previously reported[30] with the following modifications: Samples (100 μM in 50% MeOH, 50% 10 mM aqueous ammonium formate) were infused through an ESA Coulochem 5011 analytical cell (ESA Inc., Bedford, MA) by a syringe pump at a flow of 5 μL/min. A makeup flow of 50 μL/min (50% MeOH, 50% aqueous 10 mM ammonium formate) was added prior to the electrochemical cell by a Hewlett-Packard HP1050 pump (Palo Alto, CA) giving a total flow of 55 μL/min through the electrochemical cell. The electrochemical cell was controlled by an ESA

(24) De Meijere, A.; Chaplinski, V.; Gerson, F.; Merstetter, Pl; Haselbach, E. *J. Org. Chem.* **1999**, *64*, 6951. De Meirere, A.; Chaplinski, V.; Winsel, H.; Kusnetsov, M. A.; Rademacher, P.; Boese, R.; Haumann, T.; Traetteberg, M.; Schleyer, P. von R.; Zywietz, T.; Jiao, H.; Merstetter, P.; Gerson, F. *Angew. Chem., Int. Ed.* **1999**, *38*, 2430.

(25) Wang, Y.; Luttrull, D. K.; Dinnocenzo, J. P.; Goodman, J. L.; Farid, S.; Gould, I. R. *Photochem. Photobiol. Sci.* **2003**, *2*, 1169. Shaffer, C. L.; Morton, M. D.; Hanzlik, R. P. *J. Am. Chem. Soc.* **2001**, *123*, 8502. Loeppky, R. N.; Elomari, S. *J. Org. Chem.* **2000**, *65*, 96. Ha, J. D.; Lee, J.; Blackstock, S. C.; Cha, J. K. *J. Org. Chem.* **1998**, *63*, 8510. Musa, O. M.; Horner, J. H.; Shahin, H.; Newcomb, M. J. *J. Am. Chem. Soc.* **1996**, *118*, 3862.

(26) Bouchoux, G.; Alcaraz, C.; Dutuit, O.; Nguyen, M. T. *J. Am. Chem. Soc.* **1998**, *120*, 152. Nguyen, M. T.; Creve, S.; Ha, T.-Y. *Chem. Phys. Lett.* **1998**, *294*, 90.

(27) Gessner, W.; Brossi, A.; Shen, R. S.; Fritz, R. R.; Abell, C. W. *Helv. Chim. Acta* **1984**, *67*, 2037.

(28) Wu, E. Y.; Chiba, K.; Trevor, A. J.; Castagnoli, N., Jr. *Life Sci.* **1986**, *39*, 1695.

(29) Hall, L.; Murray, S.; Castagnoli, K.; Castagnoli, N., Jr. *Chem. Res. Toxicol.* **1992**, *5*, 625.

(30) Jurva, U.; Wikström, H. V.; Weidolf, L.; Bruins, A. P. *Rapid Commun. Mass Spectrom.* **2003**, *17*, 800. Jurva; U.; Bruins; A. P.; Wikström, H. V. *Rapid Commun. Mass Spectrom.* **2000**, *14*, 529.

Coulochem II potentiostat (ESA Inc., Bedford, MA). The ESA working electrode was porous graphite, and all reported cell potentials are measured vs a palladium reference electrode. The potentiostat was programmed to perform a scan from 0 to +1500 mV at a scan rate of 2 mV/s. The outlet from the ESA cell was connected to a Finnigan TSQ7000 triple stage quadrupole mass spectrometer (Finnigan MAT, San Jose, CA) equipped with an electrospray interface. Full scan spectra were acquired continuously. The delay between the electrochemical cell and the mass spectrometer was determined to be 45 s as follows: at a continuous flow of 1-cyclopropyl-1,2,3,6-tetrahydropyridine (**19**), a potential step from 0 to +650 mV was performed at the same time that the mass spectrometer was started and the delay time (45 s) for the appearance of the decyclopropylated product **30H**$^+$ was noted. Spectra could be assigned to any given potential, and the signals from the different oxidation products could be extracted from the full scan data files and plotted against the potential. Samples prepared for analysis by LC-ESI/MS/MS were infused through the electrochemical cell at the desired fixed potential. The collected perfusates (200 μL) were diluted with 800 μL of 10 mM formic acid, and 20 to 30 μL aliquots were injected onto the LC-ESI/MS/MS system.

LC-ESI/MS/MS. A Hewlett-Packard HP1050 HPLC system (Palo Alto, CA) was used for injection of samples onto a reversed-phase HPLC column (ACE 3, C18, 2.1 mm × 75 mm). The HP1050 pump was programmed to deliver a gradient composed of MeOH and 10 mM formic acid in water at a total flow of 200 μL/min. The initial gradient (10% MeOH) was increased linearly to 90% MeOH over a period of 15 min. The mobile phase then was brought back to 10% MeOH using a linear gradient. The system was allowed to equilibrate for at least 10 min between the injections.

***trans*- and *cis*-1-(2-Methylcyclopropyl)-4-phenyl-1,2,3,6-tetrahydropyridinium Oxalate [20aH$^+$·HOOCCOO$^-$ and 20bH$^+$·HOOCCOO$^-$].** To a solution of 1-formyl-4-phenyl-1,2,3,6- tetrahydropyridine[31] (3.0 g, 16 mmol) in dry THF (150 mL), Ti(*i*OPr)$_4$ (5.2 mL, 18 mmol) was added dropwise, at room temperature, followed by *n*-propylmagnesium chloride (20 mL of a 2.0 M solution in diethyl ether). The reaction mixture was stirred under reflux for 18 h during which time it slowly turned black. After cooling to room temperature, a saturated aqueous solution of ammonium chloride was added. The inorganic salts were filtrated, and the reaction mixture was extracted with ether (3 × 20 mL). The combined organic layers were washed with brine (2 × 15 mL) and dried over Na_2SO_4, and the solvent was removed under reduced pressure to give an oily mixture of the *trans*- (**20aH**$^+$) and *cis*- (**20bH**$^+$) isomers (2.7 g, 80%). The isomers were separated by neutral alumina chromatography with hexanes/EtOAc (97:3). The oxalate salts, obtained by adding a saturated ethereal solution of oxalic acid to an ethereal solution of the separated free bases, were recrystallized from MeOH/ether to give **20aH**$^+$·**HOOCCOO**$^-$ as a white, crystalline solid: mp 179−180 °C; ^{1}H NMR (500 MHz, DMSO-d_6) δ 0.50 (m, 1H), 0.94 (m, 1H), 1.03 (d, J = 6.5 Hz, 3H), 1.20 (m, 1H), 2.21 (m, 1H), 2.66 (m, 2H), 3.24 (t, J = 6.0 Hz, 2H), 3.68 (m, 2H), 6.16 (m, 1H), 7.30 (m, 1H), 7.36 (m, 2H), 7.46 (m, 2H); ^{13}C NMR (125.8 MHz, DMSO-d_6) δ 12.7, 17.2, 25.5, 45.1, 49.8, 51.7, 119.1, 125.3, 128.1, 129.1, 134.7, 139.7, 164.0. Anal. Calcd for $C_{17}H_{21}NO_4$ (303.37): C, 67.31; H, 6.98; N, 4.62. Found: C, 67.19; H, 6.81; N, 4.50. **20bH**$^+$·**HOOCCOO**$^-$ as a white, crystalline solid: mp 154−155 °C; ^{1}H NMR (500 MHz, DMSO-d_6) δ 0.21 (m, 1H), 0.75 (m, 1H), 0.93 (m, 1H), 1.18 (d, J = 6.0 Hz, 3H), 2.07 (brs, 1H), 2.57 (m, 2H), 3.00 (m, 2H), 3.45 (m, 2H), 6.17 (m, 1H), 7.26 (m, 1H), 7.35 (m, 2H), 7.45 (m, 2H); ^{13}C NMR (125.8 MHz, DMSO-d_6) δ 11.7, 12.0, 12.3, 26.7, 42.4, 50.7, 53.0, 121.0, 125.2, 127.8, 129.0, 134.6, 140.2, 162.8. Anal. Calcd for $C_{17}H_{21}NO_4$ (303.37): C, 67.31; H, 6.98; N, 4.62. Found: C, 66.93; H, 6.95; N, 4.48. An NOE experiment was conducted to distinguish between the trans and cis isomers: The doublets corresponding to the signals for the cyclopropylmethyl groups (1.01 and 1.15 ppm) were irradiated. Enhancement of the signal for the C-1 cyclopropylmethide proton (2.19 ppm), which is oriented syn to the *trans*-cyclopropylmethyl group, was observed only with irradiation of the isomer with mp 179−180 °C.

***trans*-1-(2-Phenylcyclopropyl)-4-phenylpyridinium Perchlorate (27$^+$·ClO$_4^-$).[11b]** A solution of 1-(2,4-dinitrophenyl)-4-phenylpyridinium chloride[32] (3.68 g, 10 mmol) and *trans*-2-phenylcyclopropylamine (2.74 g, 21 mmol) in anhydrous 1-butanol (60 mL) was heated under reflux overnight. The solvent was removed under reduced pressure, and water (200 mL) was added to the residue. The aqueous phase was washed with CH_2Cl_2 (5 × 50 mL), and the water was removed under reduced pressure. The MeOH (50 mL) solution of the residue was dried over Na_2SO_4 and clarified with charcoal. After filtration, the solvent was removed under reduced pressure to give the chloride salt as a yellow hygroscopic solid (1.78 g, 48%). The solid that was in MeOH (20 mL) was treated with $HClO_4$ 70% (1.5 equiv) in MeOH (1 mL), and ether was added to give **27**$^+$·**ClO$_4^-$** as white crystals (1.60 g, 43%): mp 167−168 °C; ^{1}H NMR (500 MHz, DMSO-d_6) δ 1.85 (m, 1H), 2.21 (m, 1H), 3.07 (m, 1H), 4.66 (m, 1H), 7.34 (m, 5H), 7.66 (m, 3H), 8.11 (m, 2H), 8.49 (d, J = 6.5 Hz, 2H), 9.17 (d, J = 6.5 Hz, 2H); ^{13}C NMR (125.8 MHz, CD_3OD) δ 16.4, 26.0, 49.6, 124.7, 127.3, 127.5, 128.8, 129.1, 130.3, 132.8, 134.0, 138.8, 145.4, 155.7. Anal. Calcd for $C_{20}H_{18}ClNO_4$ (371.82): C, 64.61; H, 4.88; N, 3.77. Found: C, 64.40; H, 4.63; N, 3.82.

4-Phenyl-*trans*-1-(2-phenylcyclopropyl)-1,2,3,6-tetrahydropyridinium-2,6-d_2 Oxalate [21H$^+$·HOCCOO$^-$-2,6-d_2]. To a solution of 4-phenyl-*trans*-1-(2-phenylcyclopropyl)pyridinium perchlorate **27**$^+$·**ClO$_4^-$** (594 mg, 1.6 mmol) in MeOH (50 mL) $NaBD_3CN$ (428 mg, 6.5 mmol) was added in small portions. After 1 h at room temperature, the solvent was removed under reduced pressure and the residue in water (50 mL) was extracted with CH_2Cl_2 (2 × 30 mL). The combined organic layers were dried over Na_2SO_4 and filtered, and the solvent was removed under reduced pressure. The crude product in EtOAc was filtrated through a short neutral alumina column, and the recovered free base in ether was treated with a saturated solution of oxalic acid in ether. The resulting precipitate was collected and recrystallized from MeOH/ether to give **21H**$^+$·**HOCCOO**$^-$**-2,6-d_2** as white crystals (230 mg, 39%): mp 188−189 °C; ^{1}H NMR (500 MHz, DMSO-d_6) δ 1.17 (m, 1H), 1.30 (m, 1H), 2.26 (m, 1H), 2.42 (m, 1H), 2.59 (m, 2H), 3.11 (m, 1H), 3.54 (m, 1H), 6.17 (m, 1H), 7.17 (m, 3H), 7.28 (m, 3H), 7.35 (t, J = 7.5 Hz, 2H), 7.44 (m, 2H); ^{13}C NMR (125.8 MHz, DMSO-d_6) δ 14.7, 22.8, 25.7, 47.3, 49.4, 51.4, 119.4, 125.3, 126.6, 126.7, 128.1, 128.9, 129.0, 134.7, 139.8, 140.7, 163.9. Anal. Calcd for $C_{22}H_{21}D_2NO_4$ (367.43): C, 71.92; H, 6.86; N, 3.81. Found: C, 71.74; H, 6.55; N, 3.83.

Diastereomeric Mixture of 1-[3-Phenyl-(*Z*,*E*)-propenylidinyl]-4-phenyl-1,2,3,6-tetrahydropyridinium Perchlorate (45$^+$·ClO$_4^-$) and 1-[3-Phenyl-(*E*,*E*)-propenylidinyl]-4-phenyl-1,2,3,6-tetrahydropyridinium perchlorate (48$^+$·ClO$_4^-$). To a solution of the *N*-oxides **46**/**47** (39 mg, 0.13 mmol) in CH_2Cl_2 (1 mL) TFAA (90 mL, 0.65 mmol) was added dropwise at 0 °C. After 30 min, 70% $HClO_4$ (0.2 mmol) in MeOH (0.1 mL) was added followed by addition of ether. The precipitate was recrystallized from MeOH to give a mixture of **45**$^+$·ClO$_4^-$ and **48**$^+$·ClO$_4^-$ as light yellow crystals (30 mg, 62%): mp 213 °C (dec); UV−vis (CH_3CN): λ_{max} 333 nm, ϵ 30 620; ^{1}H NMR (500 MHz, DMSO-d_6) δ 2.92 (m, 4H), 4.26 (m, 2.4H), 4.46 (m, 1.6H), 4.78 (m, 1.6H), 4.91 (m, 2.4H), 6.28 (m, 2H), 7.34−8.00 (m, 24H), 8.90 (m, 2H); ^{13}C NMR (125.8 MHz, DMSO-d_6) δ 27.7, 27.8, 47.9, 49.5, 55.2, 56.7, 117.5, 117.7, 118.1, 118.7, 125.5, 125.6, 128.5, 129.2, 129.5, 130.0, 130.9, 133.8, 133.9, 134.4, 134.5, 135.3, 139.0, 139.1, 160.1, 160.4, 168.9, 169.3. Anal. Calcd for $C_{20}H_{20}ClNO_4$ (373.83): C, 64.26; H, 5.39; N, 3.75. Found: C, 64.08; H, 5.38; N, 3.75. The ^{1}H NMR spectrum of a solution of this product (5 mg) in DMSO-d_6 (0.75 mL) containing D_2O (0.l mL) established that the starting enimiunium

(31) Kuttab, S.; Mabic, S. *J. Labelled Compd. Radiopharm.* **2002**, *45*, 813.

(32) Genisson, Y.; Mehamandonst, M.; Marazano, C.; Das, B. C. *Heterocycles* **1994**, *39*, 811.

species had hydrolyzed completely after 3 h to give an equimolar mixture of cinnamaldehyde (**32**) [δ 7.46 (m, 3H), 7.73 (m, 3H), 8.82 (dd, J = 7.7, 16.0 Hz, 1H), 9.65 (d, J = 7.5 Hz, 1H)], and the 4-phenyl-1,2,3,6-tetrahydopyridinium species **30H**$^+$ [δ 2.66 (m, 2H), 3.31 (t, J = 7.0 Hz, 2H), 2.73 (m, 2H), 6.17 (h, J = 7.0 Hz, 1H), 7.31 (m, 1H), 7.37 (m, 2H), 7.46 (m, 2H)]. Similarly, the ESI/MS spectrum of the eniminium mixture in 50:50 MeOH/10 mM aqueous ammonium formate (MH^+, m/z 274) after standing 5 h showed the complete conversion to the *N*-dealkylated compound **30H**$^+$ (MH^+, m/z 160), which was identified by comparing the corresponding PIS [MH^+, m/z 160 (25%), 30 (100%)] with that of an authentic sample **30H**$^+$**·Cl**$^-$, and cinnamaldehyde, which was identified by UV/vis diode array analysis as described in the General Methods section.

4-Phenyl-1-*trans*-(3-phenyl-2-propenyl)-1,2,3,6-tetrahydropyridinium Oxalate (49H$^+$·HOOCCOO$^-$). Cinnamyl bromide (0.17 mL, 1.2 mmol) was added at room temperature to a mixture of 4-phenyl-1,2,3,6-tetrahydropyridine (**30**, 370 mg, 2.3 mmol) and K_2CO_3 (1.6 g, 12 mmol) in acetone (20 mL). After 12 h, the mixture was filtrated, the solvent was removed under reduced pressure, and the crude product was purified by alumina chromatography with hexanes/AcOEt (80:20). The free base in ether was treated with an ethereal solution of oxalic acid to give analytically pure **49H**$^+$**·HOOCCOO**$^-$ as a white solid (301 mg, 69%): mp 216−217 °C; ^{1}H NMR (500 MHz, DMSO-d_6) δ 2.70 (m, 2H), 3.27 (t, J = 7.5 Hz, 2H), 3.71 (m, 2H), 3.80 (d, J = 8.5 Hz, 2H), 6.15 (m, 1H), 6.38 (m, 1H), 6.78 (d, J = 20 Hz, 1H), 7.35 (m, 10H); ^{13}C NMR (125.8 MHz, DMSO-d_6) δ 24.8, 48.3, 50.3, 57.5, 118.0, 120.6, 125.2, 127.1, 128.2, 128.8, 128.9, 129.1, 134.4, 136.1, 137.6, 139.1, 164.4. Anal. Calcd for $C_{22}H_{23}NO_4$ (365.43): C, 72.31; H, 6.34; N, 3.83. Found: C, 72.08; H, 6.40; N, 3.79. Treatment of the eniminium mixture described above (24 mg, 64 μmol) with $NaBH_4$ (24 mg, 0.64 mmol) gave a product that, upon workup, yielded an oxalate salt (12 mg, 51%) that was shown by mp, ^{1}H NMR, and GC-EI/MS to be identical to **49H**$^+$**·HOOCCOO**$^-$.

Acknowledgment. This work was supported by the Harvey W. Peters Research Center and AstraZeneca R&D Mölndal, Sweden. The authors thank X. Wu and K. Castagnoli who performed the LC-diode array analyses of cinnamaldehyde.

JA052048O